IEEE Access
Multidisciplinary | Rapid Review | Open Access Journal

Received January 19, 2019, accepted March 23, 2019, date of publication March 28, 2019, date of current version April 17, 2019.

Digital Object Identifier 10.1109/ACCESS.2019.2907964

Determination of L-Ascorbic Acid Using MBs-AOX/GO/IGZO/Al by Wireless Sensing System and Microfluidic Framework

JUNG-CHUAN CHOU[1], (Senior Member, IEEE), YOU-XIANG WU[1], PO-YU KUO[1], (Member, IEEE), CHIH-HSIEN LAI[1], (Member, IEEE), YU-HSUN NIEN[2], (Member, IEEE), SI-HONG LIN[1], SIAO-JIE YAN[1], AND CIAN-YI WU[1]

[1]Graduate School of Electronic Engineering, National Yunlin University of Science and Technology, Douliou 64002, Taiwan
[2]Graduate School of Chemical and Materials Engineering, National Yunlin University of Science and Technology, Douliou 64002, Taiwan

Corresponding author: Jung-Chuan Chou (choujc@yuntech.edu.tw)

This work was supported in part by Ministry of Science and Technology, Republic of China (R.O.C), under the contracts (MOST 105-2221-E-224-049, MOST 106-2221-E-224-047, and MOST 107-2221-E-224-030).

ABSTRACT In this paper, the L-ascorbic acid (L-AA) biosensor based on magnetic beads-ascorbate oxidase/graphene oxide/indium gallium zinc oxide/aluminum (MBs-AOX/GO/IGZO/Al) membrane was integrated with the potentiometric measurement system with the microfluidic framework in order to investigate the different sensing characteristics under the static condition and the dynamic condition. The L-AA biosensor showed the average sensitivity of 78.9 mV/decade (25 °C) under the static condition, and it showed the average sensitivity of 81.7 mV/decade (25 °C) at the optimal flow rate (25 μL/min). Besides, the XBee module was used to apply in the remote detection for the L-AA biosensor, and the experimental results were shown the average sensitivity of 78.7 mV/decade (25 °C). Moreover, we also investigated various experiments, such as temperature effect, hysteresis effect, and lifetime. These experimental results would be beneficial to the development of the L-AA biosensor based on electrochemical detection.

INDEX TERMS L-ascorbic acid (L-AA), graphene oxide (GO), magnetic beads (MBs), microfluidic framework, wireless sensing system.

I. INTRODUCTION

Biosensors are usually used to detect environmental chemicals in human blood or outside. The biosensors can be distinguished two main types by methods of signal generation such as bioaffinity sensors and biocatalytic biosensors. The bioaffinity sensors are defined that the biological device bound with test object to occur bioaffinitive binding result in the change of the biomolecular shape or change of physical quantities such as charge, thickness, mass, heat, or optics [1]. The biocatalytic biosensors are defined that immobilized molecules react with the test object to generate biochemical metabolites [2]. Then, it can be detected by specific electrodes, and the electronic signal can be obtained through a measurement system. At present, the two kinds of main researches in the development of biocatalytic biosensors are enzymatic biosensor and biosensor of biological cells, and the L-AA biosensor in this study belongs to an enzymatic biosensor. Graphene which is composed of the atomic of carbon, which possesses the structure of hexagonal and thickness of one carbon atom. The graphene is the excellent two-dimensional material, and it possesses the high specific surface area, thermal stability in air, good mobility of charge carriers [3], good mechanical strength [4], good thermal electrical conductivity [5], low electrical resistivity [6], and high transparency [7]. However, the above advantages of graphene are achieved according to the fabrication process of graphene-based materials, which resulted in the form of reduced graphene oxide (RGO) and graphene oxide (GO). Recently, the GO was widely applied to improve the enzymatic biosensor due to the oxygen-containing functional groups [8] and high specific surface area.

The associate editor coordinating the review of this manuscript and approving it for publication was Muhammad Omer Farooq.

Moreover, at present, the MBs can bond specific moieties for biomolecules [9] or particular biomolecules such as DNA, RNA, and protein. Therefore, the MBs were used as supports or carriers in biosensor widely such as covalent bonding method [9]–[11]. Currently, the microfluidic device was developed to integrate biosensor, which has been studied for over 20 years [12].

The microfluidic device was applied to improve the sensitivity, and it could reduce the amount of test solution [13] and even improve ion diffusion [14]. In this study, the microfluidic device was integrated with the L-AA biosensor in order to investigate the different sensing characteristic under the static condition and dynamic condition. Besides, remote real-time detection is crucial owing to the development of homecare in recent years. Table 1 showed the common communication protocols in short range network include the specifications of different protocols [15]–[18]. In order to achieve a remote detection, the biosensor integrated with an XBee module. The XBee module based on ZigBee standard, and it possesses some advantages, such as low power (30 mA Low Power), low cost, low data rate (250 kb/s), easily scaled network, and standard of wireless personal area network (WPAN) [19], [20]. Given the reasons, we selected the ZigBee module in order to apply to detection for L-AA in a long distance.

TABLE 1. The communication protocols in short range network [15]–[18].

Protocol	ZigBee	Bluetooth	NFC	6LoWPAN
Standard	IEEE 802.15.4	IEEE 802.15.1	ISO/IEC 14443 A&B,JIS X-6319- 4	IEEE 802.15.4
Frequency Bands	2.4 GHz	2.4 GHz	125 kHz, 13.56 MHz, 860 MHz	868 MHz (EU), 915 MHz (USA), 2.4 GHz (Global)
Network	WPAN	WPAN	P2P Network	WPAN
Topology	Star, Mesh, Cluster Network	Star-Bus Network	P2P Network	Star, Mesh Network
Data rate	250 kbits/s	1 Mbits/s	106 212 or 424 kbits/s	250 kbits/s
Range	10-100 m	~15-30 m	0-10 cm, 0-1 m, 10 cm-1 m	10-100 m
Power	30 mA, Low Power	30 mA, Low Power	50 mA, Low Power Very Low	Low Power Consumption
Features	Mesh Network	Low Power, Version Available	Security	Commonly Used Internal Access
Applications	This study	[16] 2009	[17] 2016	[18] 2013

II. EXPERIMEANTAL

A. MATERIALS

The polyethylene terephthalate (PET) substrate was purchased from Zencatec Corporation (Taiwan). The silver paste was purchased from Advanced Electronic Material Inc. (Taiwan). The aluminum ingots were purchased from Summit-Tech Resource Co., Ltd (Taiwan). The indium gallium zinc oxide (IGZO) target was purchased from Ultimate Materials Technology Co., Ltd. (Taiwan). The epoxy thermosetting polymer (product no. JA643) was purchased from Sil-More Industrial, Ltd. (Taiwan). The L-AA was purchased from Sigma-Aldrich Co. (U.S.A). The AOX was purchased from Sigma-Aldrich Co. (U.S.A). The hummer method was used to fabricate the GO powder. The phosphate monobasic (KH_2PO_4) powder was purchased from Darmstadt (Germany). The potassium phosphate dibasic (K_2HPO_4) powder was purchased from Katayama Chemical Co., Ltd. (Japan). The 3-glycidoxypropyl-trimethoxysilane (GPTS) was purchased from Sigma-Aldrich Co. (USA). The toluene was purchased from Sigma-Aldrich Co. (USA). The MBs solution was purchased from Quantum Biotechnology Inc. (Taiwan). The Polydimethylsiloxane (PDMS) silicone elastomer and curing agent were purchased from Dow Corning Inc. (U.S.A). The N - (3 – Dimethylaminopropyl) – N - ethylcarbodiimide hydrochloride (EDC) was purchased from Sigma-Aldrich Co. (U.S.A).

B. FABRICATION OF IGZO/AL MEMBRANES

The PET substrate (dimension: 3 cm × 4 cm) was cleaned by nitrogen gun, alcohol and deionized (D. I.) water. Afterwards, the oven was used to remove the steam on a PET substrate at 100 °C for 10 min. Then, the cleaning steps of the PET substrate were finished. We adopted the screen printing technology to fabricate reference electrodes and conductive wires on the PET substrate. Next, the thermal evaporation system was adopted to deposit aluminum (Al) membranes onto the extremity of conductive wires. After that, we adopted radio frequency (R. F.) sputtering system to deposit IGZO membranes onto the Al membranes at 3 mTorr working pressure, power of 40 W and flow rates of 16/2 for Ar/O_2 (sccm). Lastly, the epoxy which was used as an insulation layer, and defined the size of sensing window was printed on the substrate by screen printing technology, and the flexible arrayed IGZO/Al membranes were successfully fabricated.

C. MBS-AOX SOLUTION

Firstly, the ascorbate oxidase (AOX) solution contained 200 μl PBS solution (50 mM) and 250 U AOX, which was mixed with MBs in order to fabricate MBs-AOX solution. The MBs solution (400 μl) which sucked out by micropipette were separated into the MBs and maintenance liquid by DynaMag magnet device. After that, the PBS solution was used to clean the MBs. On the other hand, the EDC (10 mg) mixed with PBS solution (1 ml) was shaken by a stirrer for 10 min. Afterwards, the EDC (100 μl) solution mixed with MBs were shaken by a stirrer for 30 min. Then, we separated the MBs and EDC solution by DynaMag magnet device. Finally, we mixed the AOX solution and MBs to fabricate the MBs-AOX solution, and we stored the MBs-AOX in a

refrigerator at 4 °C for 1 day, the MBs-AOX solution was successfully prepared.

D. IMMOBILIZATION OF MBS-AOX

Firstly, in order to immobilize AOX more stable and increased specific surface area, we deposited 0.3 wt% GO on the IGZO membranes. Next, the cross-linking agent included 100 μl GPTS and 400 μl toluene were dropped on the GO membranes to immobilize enzyme by covalent bonding method. Then, the samples were baked by an oven at 80 °C for 1 h. Afterwards, in order to remove unlinked cross-linking layer, the samples were immersed in the PBS solution. Finally, the MBs-AOX solution was dropped on the cross-linking layer, and we stored the samples in refrigerator at 4 °C. The schematic diagram of the MBs-AOX/GO/IGZO/Al L-AA biosensor was shown in Fig. 1.

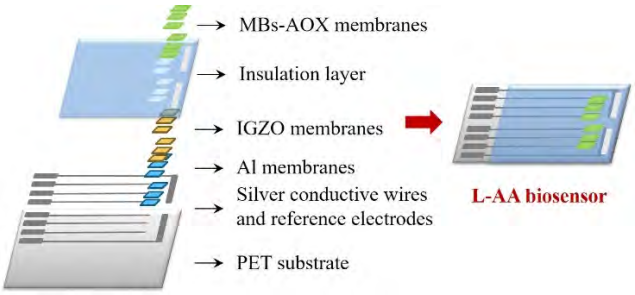

FIGURE 1. The schematic diagram of the MBs-AOX/GO/IGZO/Al L-AA biosensor.

E. MEASUREMENT SYSTEMS

According to the literatures [21]–[24], in this study, a potentiometric measurement system was fabricated in order to detect concentrations of L-AA under the static condition and dynamic condition. Besides, there is a difference between this experiment and literatures, it consists of a microfluidic device and an injection pump. In order to fabricate the microfluidic device, the epoxy was used to define the shape of microfluidic device. The PDMS was mixed with curing agent, which weight ratio was 10:1. Next, the PDMS mixture was poured into a microfluidic master mold to fabricate the microfluidic device. Afterward, we used the upper acrylic sheet layer and lower acrylic sheet layer to fix the microfluidic device. For more details, the schematic diagrams of the microfluidic device were referred to our previous study by the same group [25, Fig. 4], were shown in Fig. 2. Finally, the magnetic beads-ascorbate oxidase/graphene oxide/indium gallium zinc oxide/aluminum (MBs-AOX/GO/IGZO/Al) L-AA biosensor was integrated with the microfluidic device, the injection pump and the potentiometric measurement system in order to measure the characteristics of biosensor under the dynamic conditions. The photo of the potentiometric measurement system with the microfluidic framework for the L-AA biosensor was shown in Fig. 3.

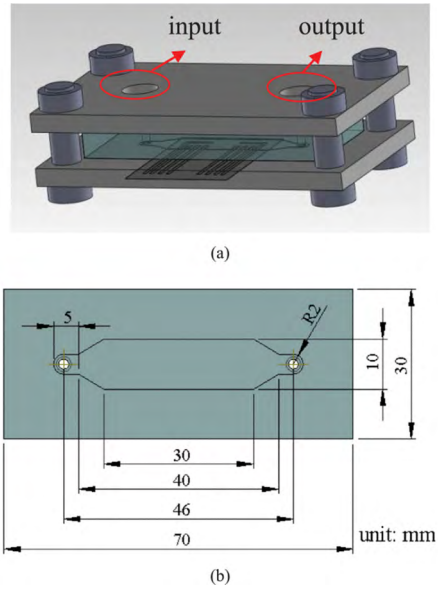

FIGURE 2. The schematic diagrams of the microfluidic device. (a) The microfluidic device and the biosensor under measuring. (b) The drawing of the microfluidic channel [25].

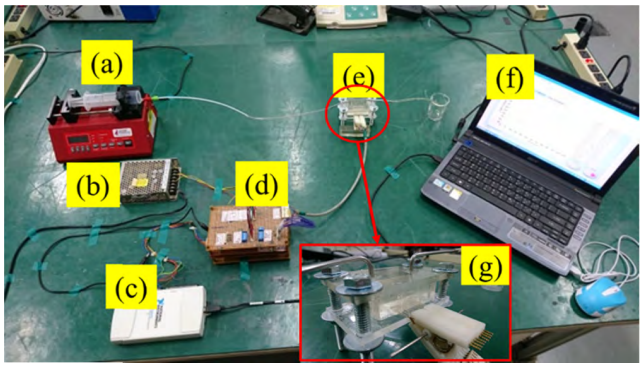

FIGURE 3. The potentiometric measurement system with the microfluidic framework for the MBs-AOX/GO/IGZO/Al L-AA biosensor. (a) The injection pump, (b) the power supply, (c) the data acquisition card, (d) the readout circuit, (e) the microfluidic device, (f) the computer, and (g) the close-up image of the biosensor during measuring.

The wireless sensing system was fabricated according to the literatures [26]–[28]. The XBee device includes an XBee coordinator and an XBee router. The measurement signals were received, which were transmitted to the XBee router through Arduino Mega 2560. Afterwards, the measurement signals were wirelessly transmitted to the XBee coordinator. Next, the measurement signals were transmitted to the computer, and the measurement signals were shown on the computer screen through LabVIEW software. The photo of the wireless sensing system was shown in Fig. 4.

F. SETTING OF THERMOSTATIC WATER BATH

In order to investigate the effects of temperatures for MBs-AOX/GO/IGZO/Al L-AA biosensor, the thermostatic water bath, temperature controller (Model: TAIE FY-400, Taiwan), and digital thermometer (Model: TM-906A, Taiwan) were used to carry out the temperature effects.

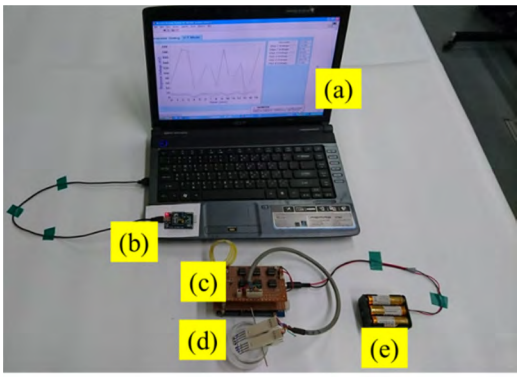

FIGURE 4. The wireless sensing system for the MBs-AOX/GO/IGZO/Al L-AA biosensor. (a) The computer, (b) the XBee device, (c) the readout circuit and the XBee device, (d) the biosensor and the solution, and (e) the batteries.

As shown in Fig. 5, it could be seen that the internal setting such as (a) the temperature controller (b) the digital thermometer (c) the water bath, and (d) the biosensor. The thermostatic water bath was used to soak the glass jar of L-AA solution in hot water to warm it up. Besides, the digital thermometer was used to calibrate temperature for L-AA solution. The temperature difference between the digital thermometer and the thermostatic water bath was about 3 °C. After the temperature was achieved stable state, the MBs-AOX/GO/IGZO/Al L-AA biosensor was immersed in the different L-AA solutions, which the temperatures were set from 25 °C to 65 °C.

FIGURE 5. The setting of thermostatic water bath for temperature effects. (a) The temperatures controller, (b) digital thermometer, (c) the water bath, and (d) the biosensor.

III. RESULTS AND DISCUSSION

A. SENSING CHARACTERISTICS FOR L-AA BIOSENSORS BASED ON DIFFERENT MEASUREMENT SYSTEMS

In this study, the MBs-AOX/GO/IGZO/Al L-AA biosensor based on an enzymatic potentiometric biosensor. The sensing mechanism is following formulas (1) and (2) [29]:

$$\mathrm{E} = E^0 - 2.303\frac{RT}{F}pH \tag{1}$$

$$\text{L-ascorbic acid} \xrightarrow{\text{Ascorbate oxidase}} \text{Dehydro-L-ascorbic acid} + 2\mathrm{H}^+ + 2\mathrm{e}^- \tag{2}$$

where E is the electromotive force (EMF), E^0 is the standard potential of the reference electrode, R is the gas constant, T is the temperature in kelvins, and F is the Faraday's constant. pH is the pH of the electrolyte. In addition, the rate of change in E with respect to the pH of the solution is affected by the membrane [30]. The formula (3) is related to the sensitivity of a biosensor directly. The formula (3) is shown as follows:

$$\frac{\partial \mathrm{E}}{\partial \mathrm{pH}} = 2.303\frac{RT}{F} \tag{3}$$

According to the Nernst equation, the concentration of hydrogen ions in the solution affected the electromotive of the working electrode. As shown in formula (2), the enzymatic catalytic reaction showed that L-Ascorbic acid converted into Dehydro-L-Ascorbic acid, two hydrogen ions, and two electrons. The pH in the micro surrounding the sensing membrane is changed owing to the change of H^+, thereby generating the different electromotive forces to achieve detection of L-AA.

In this experiment, the experiments were divided into two parts which were dynamic condition and static condition. Because it could be confirmed whether the L-AA biosensor could detect the L-AA concentration in human blood, the L-AA biosensor integrated with the potentiometric measurement system with the microfluidic framework. The dynamic experiment results were shown in Table 2 and Fig. 6, it could be found that the flow rates of the injection pump were set at 5μL, 10μL, 15μL, 20μL, 25μL and 30μL, respectively. From Fig. 6 and Table 2, it could be found that the average sensitivities were 79.4 mV/decade, 79.7 mV/decade, 79.9 mV/decade, 81.1 mV/decade, 81.7 mV/decade, and 80.0 mV/decade, respectively. Besides, the linearities were 0.997, 0.996, 0.995, 0.998, 0.999, and 0.993, respectively (25 °C).

TABLE 2. The average sensitivities and linearities of the MBs-AOX/GO/IGZO/Al L-AA biosensor at different flow rates.

Flow rates (μL/min)	Average sensitivity (mV/decade)	Linearity
5	79.4	0.997
10	79.7	0.996
15	79.9	0.995
20	81.1	0.998
25	81.7	0.999
30	80.0	0.993

According to the experimental results, it could be observed that the average sensitivities were increased with increasing flow rate. The reason is attributed to the diffusion resistance and catalyzed reaction rate. The diffusion resistance of membrane depends on the diffusion layer of mem-

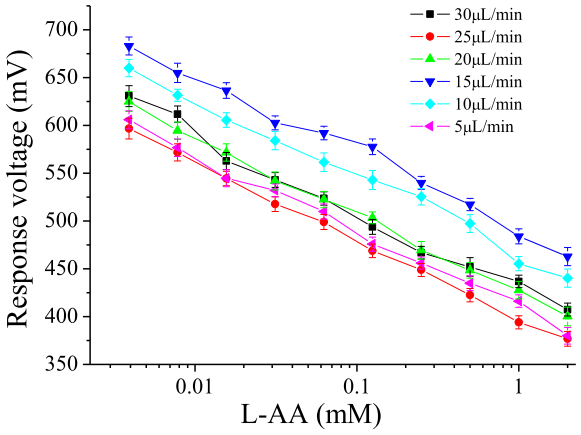

FIGURE 6. The average sensitivity and linearity of the MBs-AOX/GO/IGZO/Al L-AA biosensor under the different flow rates conditions.

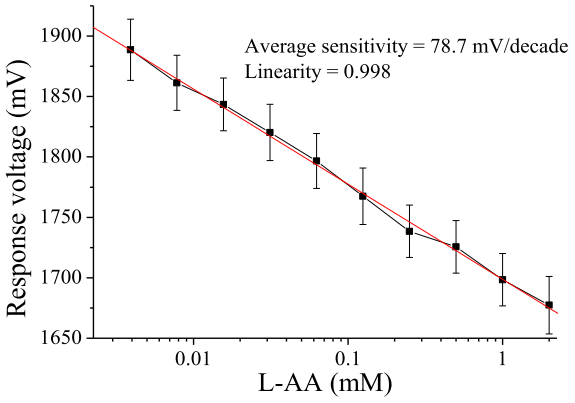

FIGURE 7. The curves of response voltage for the MBs-AOX/GO/IGZO/Al L-AA biosensor measured by the wireless sensing system.

brane under dynamic fluid. The diffusion layer of membrane becomes thinner when the flow rate increases [31]. This phenomenon results in the catalyzed reaction can be promoted to the generation of more hydrogen ions, thereby enhancing the sensing characteristics of the membrane. Because AOX has not enough time to induce catalyzed reactions under high flow rate [24], [21], the sensitivity of MBs-AOX/GO/IGZO/Al membrane decreased when the flow rate beyond 25μL/min. However, the sensitivity of the biosensor is attributed to the several factors, such as the diffusion resistance within interface between solid and liquid, the enzyme loading, and temperature [31]–[33]. At room temperature (25 °C), the best response voltage is in 15μL/min, but the sensitivity and linearity are no better than the sensing characteristics in 25μL/min. In conclusion, the optimal flow rate is the 25μL/min, which is suitable for the MBs-AOX/GO/IGZO/Al L-AA biosensor. The optimal average sensitivity was 81.7 mV/decade (25 °C) under the 25 μL/min flow rate.

Moreover, the remote detection results were shown in Fig. 7, it could be found that the average sensitivity of 78.7 mV/decade (25 °C) and linearity of 0.998. That data were similar to the data which were measured by potentiometric measurement system. It could be confirmed that the wireless sensing system could be applied in detection of biosensor. Now, the wireless sensing system has become the trend of modern sensor.

B. SENSING CHARACTERISTICS FOR MBS-AOX/GO/IGZO/AL L-AA BIOSENSOR AT DIFFERENT TEMPERATURES

According to the work [34], Sardarinejad *et al.* proposed that the temperature of solution was increased, which resulted in viscosity decreased and the mobility of ions increased. Besides, the dissociation rate could be improved to be quickened, which resulted in the number of ions increased in the solution. According to the Nernst equation, the measured potential changed which produced between the reference electrode and the working electrode, which were relied on the temperature.From the Nernst equation, the potential on the electrode can be influenced by changing the temperature, thereby changing the average sensitivity of the biosensor. Therefore, the temperature effects were investigated through the temperature coefficient of the average sensitivity in this study.

The experimental results were shown in Fig. 8 and Table 3, we could observe that the average sensitivity and the linearity of the MBs-AOX/GO/IGZO/Al L-AA biosensor were 78.9 mV/decade and 0.997, respectively at room temperature (25 °C). Besides, the average sensitivity could be enhanced

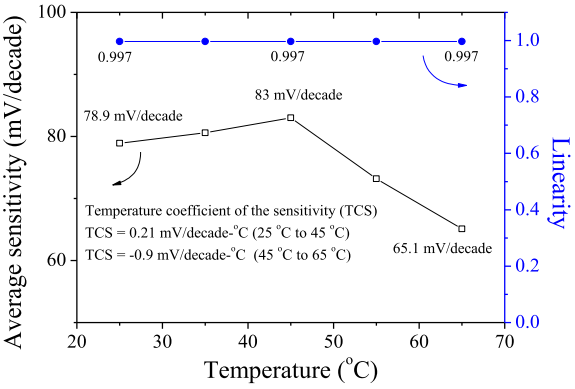

FIGURE 8. The temperatures effects for sensing characteristics of the MBs-AOX/GO/IGZO/Al L-AA biosensor.

TABLE 3. The sensing characteristics of the MBs-AOX/GO/IGZO/Al L-AA biosensor under conditions of different temperatures.

Temperatures of solution (°C)	Average sensitivity (mV/decade)	Linearity
25	78.9	0.997
35	80.6	0.997
45	83.0	0.997
55	73.2	0.997
65	65.1	0.997

with temperature increased in the range from 25 °C to 45 °C, the temperature coefficient was about 0.21 mV/decade-°C. Because the mobility of the ions in solution depends on the temperature of the solution [35], the increase in mobility of the ions causes the rate of adsorption-desorption to accelerate. Therefore, the average sensitivity of the biosensor increased at the temperature from 25 °C to 45 °C. However, the average sensitivity was quickly decreased when the temperature was increased in the range from 55 °C to 65 °C, whose temperature coefficient was about −0.9 mV/decade-°C. It could be attributed to effect of temperature on ascorbate oxidase activity. Because AOX enters the half-time of denaturation at 55 °C according to the literature [36], [37], AOX activity is decreased at the temperature exceeded 45 °C. When the temperature was continuously increased, thereby resulting in decreasing in the sensitivity of the MBs-AOX/GO/IGZO/Al L-AA biosensor.

C. LIFETIME AND DECAY RATE FOR MBS-AOX/GO/IGZO/AL L-AA BIOSENSOR

In this study, the lifetime was defined as the time that relative average sensitivity fell below 15 % during a period. The relative average sensitivity was indicated the $S_{test}/S_{initial}$, where S_{test} was indicated the average sensitivity in the test and $S_{initial}$ was indicated the average sensitivity in the initial test. In this experiment, experimental temperatures, which were divided into 25 °C and 45 °C, were used to carry out the temperatures effects, and the samples were saved in the refrigerator at 4 °C when the samples are not in use. Moreover, the decay rate was indicated that the average sensitivity was decayed with time. From section B, the L-AA biosensor showed the best average sensitivity at 45 °C. However, the average sensitivity was decreased when the temperature exceeded 45 °C. It could be confirmed that each enzyme has a suitable range of temperature. In section C, the decay rates of L-AA biosensor were investigated at 25 °C and 45 °C within 28 days.

From Fig. 9 and Table 4, the average sensitivity at 25 °C was decreased with time. On the initial day, the L-AA biosensor showed average sensitivity of the 78.9 mV/decade and linearity of 0.997. The average sensitivity was decreased until the 28th day. The L-AA biosensor showed average sensitivity of the 67.2 mV/decade, and that value was 85.1% of average sensitivity of the initial test. From Fig. 9 and Table 5, the average sensitivity at 45 °C was also decreased with time. On the initial day, the L-AA biosensor showed average sensitivity of the 83.0 mV/decade and linearity of 0.997. The average sensitivity was decreased until the 28th day. The MBs-AOX/GO/IGZO/Al L-AA biosensor showed average sensitivity of the 31.6 mV/decade, and that value was 38.0 % of the average sensitivity of the initial test.

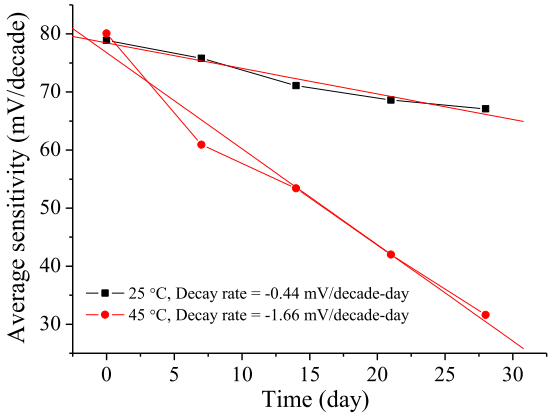

FIGURE 9. The decay rates of the MBs-AOX/GO/IGZO/Al L-AA biosensor within 28 days at 25 °C and 45 °C, respectively.

TABLE 4. Sensing characteristics of the MBs-AOX/GO/IGZO/Al L-AA biosensor at 25 °C within 28 days.

Days	Average sensitivity (mV/decade)	Linearity
Initial	78.9	0.997
7	75.9	0.997
14	71.2	0.996
21	68.7	0.997
28	67.2	0.995

TABLE 5. The sensing characteristics of the MBs-AOX/GO/IGZO/Al L-AA biosensor at 45 °C within 28 days.

Days	Average sensitivity (mV/decade)	Linearity
Initial	83.0	0.997
7	60.9	0.998
14	53.4	0.995
21	42.0	0.997
28	31.6	0.995

Through this experiment, it could be found that the lifetime of the L-AA biosensor was about 28 days, its decay rate was detected to be −0.44 mV/decade-day at 25 °C. Moreover, the lifetime of the L-AA biosensor was about 7 days, its decay rate was detected to be −1.66 mV/decade-day at 45 °C. It could be found that the MBs-AOX/GO/IGZO/Al L-AA biosensor the best average sensitivity at 45 °C, but the lifetime of L-AA biosensor was decreased a lot.

D. HYSTERESIS EFFECT OF MBS-AOX/GO/IGZO/AL L-AA BIOSENSOR

In this study, we investigated the hysteresis effect to confirm whether the L-AA biosensor can produce the right trend of response voltage after the difference of previous concentration. The experimental results were shown as follow. The cycle of hysteresis was set 0.03-0.007-0.03-0.125-0.03 mM, and this range consisted of scurvy concentration (0.007 mM), normal concentration (0.03 mM) and saturation concentration (0.125 mM) in human blood [38].

Figure 10 presented the hysteresis width of L-AA biosensor was 11.6 mV, and this value was the best result for AOX/IGZO/Al membrane. It could be found that the AOX/IGZO/Al L-AA biosensor possessed a memory effect.

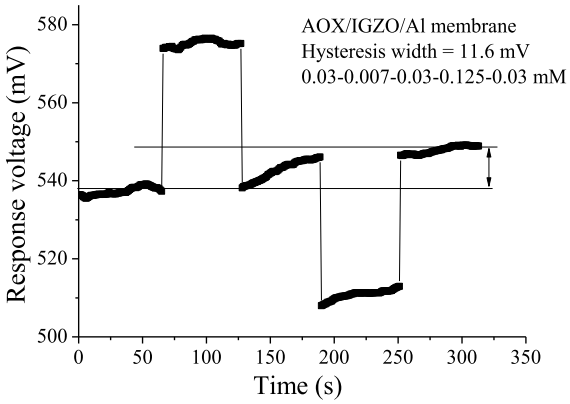

FIGURE 10. The hysteresis effect of the L-AA biosensor based on AOX/IGZO/Al membrane in L-AA solutions during the cycle of 0.03-0.007-0.03-0.125-0.03 mM.

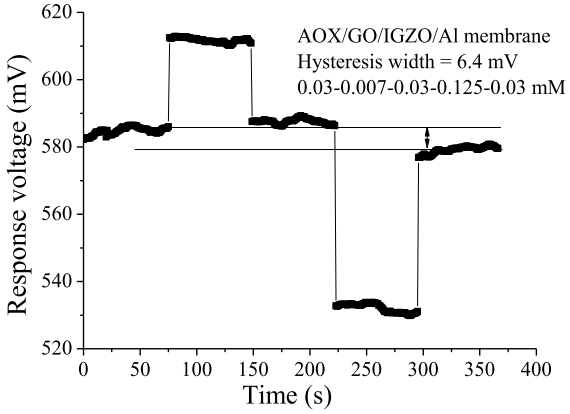

FIGURE 11. The hysteresis effect of the L-AA biosensor based on AOX/GO/IGZO/Al membrane in L-AA solutions during the cycle of 0.03-0.007-0.03-0.125-0.03 mM.

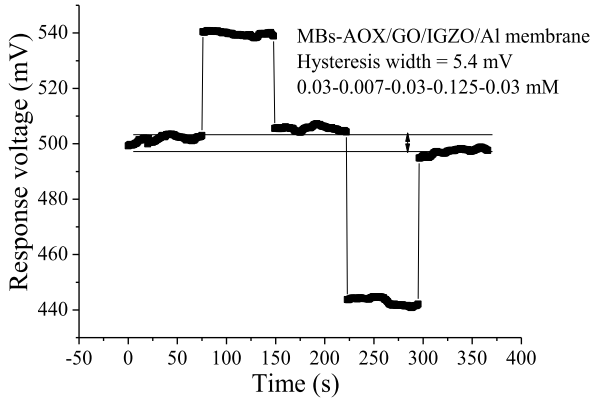

FIGURE 12. The hysteresis effect of the L-AA biosensor based on MBs-AOX/GO/IGZO/Al membrane in L-AA solutions during the cycle of 0.03-0.007-0.03-0.125-0.03 mM.

Actually, an excellent biosensor should not have any memory effect. For this reason, the GO was used to modify the AOX/IGZO/Al biosensor, and the experiment which presented the hysteresis width of 6.4 mV was shown in Fig. 11. From this experiment, it could be found that the characteristic of AOX/GO/IGZO/Al membrane was better than AOX/IGZO/Al membrane. This hysteresis effect of improvement could be attributed to these properties of GO such as high specific surface area and oxygen-containing functional groups [39]–[41]. The property of GO could make the enzyme and hydrogen ion be adsorbed on the sensing membrane well. On the other hand, we also investigated the hysteresis effect of MBs-AOX/GO/IGZO/Al sensing membrane, the experimental result was shown in Fig. 12. The experimental results are obtained the better properties; it could be attributed to not only property of GO but also MBs.

IV. CONCLUSION

In this study, various experiments such as dynamic detection, remote detection, temperature effect, hysteresis effect and lifetime carry out in order to confirm the sensing characteristics of the MBs-AOX/GO/IGZO/Al L-AA biosensor. According to the dynamic experiment results, it could be confirmed that the average sensitivity was improved from 78.9 mV/decade to 81.7 mV/decade due to the improvement of ion diffusion. Besides, the wireless sensing system based on the XBee devices was successfully applied in detection of the L-AA biosensor, and the result was similar to the value which was measured by the potentiometric measurement system. Moreover, we also found that the L-AA biosensor possessed high average sensitivity at 45 °C, but the lifetime was decreased quickly. Finally, the hysteresis width was found that it could be improved from 11.6 mV to 5.4 mV through hysteresis effect experiments. Therefore, the MBs-AOX/GO/IGZO/Al L-AA biosensor is a promising device for detecting L-AA.

REFERENCES

[1] P. Zhang, L. Liu, Y. He, Y. Ji, J. Guo, and H. Ma, "Temperature-regulated surface plasmon resonance imaging system for bioaffinity sensing," *Plasmonics*, vol. 11, no. 3, pp. 771–779, Jun. 2016.
[2] J. Raba *et al.*, "Analytical biosensors for the pathogenic microorganisms determination," *Plasmonics*, vol. 1, pp. 227–238, Dec. 2013.
[3] J. Ping, J. Wu, Y. Wang, and Y. Ying, "Simultaneous determination of ascorbic acid, dopamine and uric acid using high-performance screen-printed graphene electrode," *Biosens. Bioelectron.*, vol. 34, pp. 70–76, Jan. 2012.
[4] C. Lee, X. Wei, J. W. Kysar, and J. Hone, "Measurement of the elastic properties and intrinsic strength of monolayer graphene," *Science*, vol. 321, no. 5887, pp. 385–388, Jul. 2008.
[5] E. Pop, D. Mann, Q. Wang, K. Goodson, and H. Dai, "Thermal conductance of an individual single-wall carbon nanotube above room temperature," *Nano Lett.*, vol. 6, pp. 96–100, Dec. 2005.
[6] A. K. Geim and K. S. Novoselov, "The rise of graphene," *Nature Mater.*, vol. 6, no. 3, pp. 183–191, Mar. 2007.
[7] G. Hassink *et al.*, "Transparency of graphene for low-energy electrons measured in a vacuum-triode setup," *APL Mater.*, vol. 3, no. 7, Jul. 2015, Art. no. 076106.
[8] J. Zhang *et al.*, "Graphene oxide as a matrix for enzyme immobilization," *Langmuir*, vol. 26, pp. 6083–6085, Mar. 2010.
[9] L. Reverté, B. Prieto-Simón, and M. Campàs, "New advances in electrochemical biosensors for the detection of toxins: Nanomaterials, magnetic beads and microfluidics systems. A review," *Anal. Chim. Acta*, vol. 908, pp. 8–21, Feb. 2016.
[10] S. Kiralp, A. Topcu, G. Bayramoglu, M. Y. Arica, and L. Toppare, "Alcohol determination via covalent enzyme immobilization on magnetic beads," *Sens. Actuators B, Chem.*, vol. 128, pp. 521–528, Jan. 2008.
[11] A. Sassolas, A. Hayat, and J.-L. Marty, "Immobilization of enzymes on magnetic beads through affinity interactions," in *Immobilization of Enzymes and Cells*, vol. 1051, J. M. Guisan, Ed., 3rd ed. New York, NY, USA: Humana Press, 2013, pp. 139–148.

[12] K.-I. Miyamoto, H. Ichimura, T. Wagner, M. J. Schöning, and T. Yoshinobu, "Chemical imaging of the concentration profile of ion diffusion in a microfluidic channel," *Sens. Actuators B, Chem.*, vol. 189, pp. 240–245, Dec. 2013.
[13] Y.-C. Tan, J. S. Fisher, A. I. Lee, V. Cristini, and A. P. Lee, "Design of microfluidic channel geometries for the control of droplet volume, chemical concentration, and sorting," *Lab Chip*, vol. 4, pp. 292–298, Jul. 2004.
[14] Q. Pu, J. Yun, H. Temkin, and S. Liu, "Ion-enrichment and ion-depletion effect of nanochannel structures," *Nano Lett.*, vol. 4, pp. 1099–1103, May 2004.
[15] S. Al-Sarawi, M. Anbar, K. Alieyan, and M. Alzubaidi, "Internet of Things (IoT) communication protocols: Review," in *Proc. ICIT*, Amman, Jordan, 2017, pp. 685–690.
[16] Y.-H. Liao and J.-C. Chou, "Potentiometric multisensor based on ruthenium dioxide thin film with a bluetooth wireless and Web-based remote measurement system," *IEEE Sensors J.*, vol. 9, pp. 1887–1894, Dec. 2009.
[17] A. DeHennis, S. Getzlaff, D. Grice, and M. Mailand, "An NFC-enabled CMOS IC for a wireless fully implantable glucose sensor," *IEEE J. Biomed. Health Inform.*, vol. 20, no. 1, pp. 18–28, Jan. 2016.
[18] S.-J. Jung and W.-Y. Chung, "Non-intrusive healthcare system in globalmachine-to-machine networks," *IEEE Sensors J.*, vol. 13, no. 12, pp. 4824–4830, Dec. 2013.
[19] M. Javadi, S. Sheikhaei, A. S. Kashi, and H. Pourmodheji, "Design of a direct conversion ultra low power ZigBee receiver RF front-end for wireless sensor networks," *Microelectron. J.*, vol. 44, pp. 347–353, Apr. 2013.
[20] W.-T. Sung and K.-Y. Chang, "Health parameter monitoring via a novel wireless system," *Appl. Soft Comput.*, vol. 22, pp. 667–680, Sep. 2014.
[21] J.-C. Chou *et al.*, "The characteristic analysis of IGZO/Al pH sensor and glucose biosensor in static and dynamic measurements," *IEEE Sensors J.*, vol. 16, no. 23, pp. 8509–8516, Dec. 2016.
[22] J.-C. Chou *et al.*, "Data fusion and fault diagnosis for flexible arrayed pH sensor measurement system based on LabVIEW," *IEEE Sensors J.*, vol. 14, no. 5, pp. 1405–1411, May 2014.
[23] J.-C. Chou *et al.*, "Characterization of flexible arrayed pH sensor based on nickel oxide films," *IEEE Sensors J.*, vol. 18, no. 2, pp. 605–612, Nov. 2017.
[24] J. C. Chou *et al.*, "Flexible arrayed enzymatic l-ascorbic acid biosensor based on IGZO/Al membrane modified by graphene oxide," *IEEE Trans. Nanotechnol.*, vol. 17, no. 3, pp. 452–459, May 2018.
[25] S.-C. Tseng *et al.*, "Research of non-ideal effect and dynamic measurement of the flexible-arrayed chlorine ion sensor," *IEEE Sensors J.*, vol. 16, no. 12, pp. 4683–4690, Jun. 2016.
[26] J.-C. Chou *et al.*, "Wireless sensing system for flexible arrayed potentiometric sensor based on XBee module," *IEEE Sensors J.*, vol. 16, no. 14, pp. 5588–5595, Jul. 2016.
[27] J. C. Chou *et al.*, "Fabrication and characteristic analysis of a remote real-time monitoring applied to glucose sensor system based on microfluidic framework," *IEEE Sensors J.*, vol. 15, no. 6, pp. 3234–3240, Jun. 2015.
[28] J.-C. Chou, R.-T. Chen, Y.-H. Liao, J.-S. Chen, M.-S. Huang, and H.-T. Chou, "Dynamic and wireless sensing measurements of potentiometric glucose biosensor based on graphene and magnetic beads," *IEEE Sensors J.*, vol. 15, no. 10, pp. 5718–5725, Oct. 2015.
[29] H. Wang and S. Mu, "Bioelectrochemical response of the polyaniline ascorbate oxidase electrode," *J. Electroan. Chem.*, vol. 436, nos. 1–2, pp. 43–48, Oct. 1997.
[30] H. Nakazawa, R. Otake, M. Futagawa, F. Dasai, M. Ishida, and K. Sawada, "High-sensitivity charge-transfer-type pH sensor with quasi-signal removal structure," *IEEE Trans. Electron. Devices*, vol. 61, no. 1, pp. 136–140, Jan. 2014.
[31] A. Samphao, P. Butmee, J. Jitcharoen, L. Švorc, G. Raber, and K. Kalcher, "Flow-injection amperometric determination of glucose using a biosensor based on immobilization of glucose oxidase onto Au seeds decorated on core Fe_3O_4 nanoparticles," *Talanta*, vol. 142, pp. 35–42, Sep. 2015.
[32] C. S. Pundir, S. Jakhar, and V. Narwal, "Determination of urea with special emphasis on biosensors: A review," *Biosens. Bioelectron.*, vol. 123, pp. 36–50, Jan. 2019.
[33] W. Nouira *et al.*, "Enhancement of enzymatic IDE biosensor response using gold nanoparticles. Example of the detection of urea," *Electroanalysis*, vol. 24, pp. 1088–1094, May 2012.
[34] A. Sardarinejad, D. K. Maurya, M. Khaled, and K. Alameh, "Temperature effects on the performance of RuO_2 thin-film pH sensor," *Sens. Actuators, A Phys.*, vol. 233, pp. 414–421, Sep. 2015.
[35] J. J. Barron and C. Ashton, "The effect of temperature on conductivity measurement," Reagecon Diagnostics Ltd., Shannon Free Zone, County Clare, Ireland, Tech. Rep. TSP-07, no. 3, pp. 1–5. [Online]. Available: https://www.camlab.co.uk/originalimages/sitefiles/Tech_papers/TempCondMeas.pdf
[36] M. Maccarrone and G. D'Andrea, M. L. Salucci, L. Avigliano, and A. Finazzi-Agrò, "Temperature, pH and UV irradiation effects on ascorbate oxidase," *Phytochemistry*, vol. 32, pp. 795–798, Mar. 1993.
[37] D. K. Kannoujia, S. Kumar, and P. Nahar, "Covalent immobilization of ascorbate oxidase onto polycarbonate strip for L-ascorbic acid detection," *J. Biosci. Bioeng.*, vol. 114, pp. 402–404, Jun. 2012.
[38] C. Pacier and D. M. Martirosyan, "Vitamin C: Optimal dosages, supplementation and use in disease prevention," *Funct. Foods Health Disease*, vol. 5, pp. 89–107, Mar. 2015.
[39] S. N. A. M. Yazid, I. M. Isa, S. A. Bakar, N. Hashim, and S. A. Ghani, "A review of glucose biosensors based on graphene/metal oxide nanomaterials," *Anal. lett.*, vol. 47, pp. 1821–1834, Mar. 2014.
[40] S. Chowdhury and R. Balasubramanian, "Recent advances in the use of graphene-family nanoadsorbents for removal of toxic pollutants from wastewater," *Adv. Colloid Interface Sci.*, vol. 204, pp. 35–36, Feb. 2014.
[41] H. L. Tan, F. Denny, M. Hermawan, R. J. Wong, R. Amal, and Y. H. Ng, "Reduced graphene oxide is not a universal promoter for photocatalytic activities of TiO_2," *J. Materiomics*, vol. 3, pp. 51–57, Mar. 2017.

JUNG-CHUAN CHOU (SM'18) was born in Tainan, Taiwan, in 1954. He received the B.S. degree in physics from the Kaohisung Normal College, Kaohsiung, Taiwan, in 1976, the M.S. degree in applied physics from Chung Yuan Christian University, Chungli, Taiwan, in 1979, and the Ph.D. degree in electronics from National Chiao Tung University, Hsinchu, Taiwan, in 1988. He taught at Chung Yuan Christian University, from 1979 to 1991. Since 1991, he has been an Associate Professor with the Department of Electronic Engineering, National Yunlin University of Science and Technology, Yunlin, Taiwan, where he has been a Professor, since 2010, was the Dean of the Office of Technology Cooperation, from 1997 to 2002, was the Chief Secretary, from 2002 to 2009, the Director of Library, from 2009 to 2010, and was the Director of Office of Research and Development, from 2010 to 2011. From 2013 to 2018, he was the Director of Administration at the Testing Center for Technological and Vocational Education, and since 2018, he has been the Deputy Director of Headquarter at the Testing Center for Technological and Vocational Education. From 2011 to 2017, he was a Distinguished Professor with the Department of Electronic Engineering, National Yunlin University of Science and Technology, where he has been a Lifetime Chair Professor with the Department of Electronic Engineering, since 2018. His research interests include sensor material and device, biosensor and systems, microelectronic engineering, optoelectronic engineering, solar cell, and solid-state electronics.

YOU-XIANG WU was born in Taichung, Taiwan, in 1994. He received the B.S. degree in electro-optical engineering from National Formosa University, Yunlin, Taiwan, in 2016, and the M.S. degree in electronic engineering from the National Yunlin University of Science and Technology, Yunlin, in 2018. His areas of research are the biosensors included their applications and characterization.

PO-YU KUO (M'13) was born in Taichung, Taiwan, in 1980. He received the M.S. and Ph.D. degrees in electrical engineering from The University of Texas at Dallas, in 2006 and 2011, respectively. In 2013, he joined the Department of Electronic Engineering, National Yunlin University of Science and Technology, Yunlin, Taiwan, where he is currently an Assistant Professor. His research interests include the analog circuits, power management circuits, and analog circuit model analysis.

CHIH-HSIEN LAI (M'17) was born in Taichung, Taiwan, in 1968. He received the B.S. and M.S. degrees in electrical engineering and the Ph.D. degree in photonics and optoelectronics from National Taiwan University, Taipei, Taiwan, in 1990, 1992, and 2010, respectively. He was with the telecommunications industry for a number of years. He was an Assistant Professor with the Department of Electronic Engineering, Hwa Hsia Institute of Technology, Taipei, from 2004 to 2012. In 2012, he joined the Department of Electronic Engineering, National Yunlin University of Science and Technology, Yunlin, Taiwan, where he is currently a Professor. His current research interests include the optical and terahertz guided-wave structures, nanophotonic devices, and optoelectronic devices.

YU-HSUN NIEN (M'19) received the Ph.D. degree from the Department of Materials Science and Engineering, Drexel University, Philadelphia, PA, USA, in 2000. He is currently a Professor with the Department of Chemical and Materials Engineering and the Deputy Dean of the Office of International Affairs, National Yunlin University of Science and Technology, Yunlin, Taiwan. His research interest includes materials engineering.

SI-HONG LIN was born in Taichung, Taiwan, in 1995. He received the B.S. degree from the Department of Electronic Engineering, National Yunlin University of Science and Technology, Yunlin, Taiwan, in 2017, where he is currently pursuing the master's degree with the Graduate School of Electronic Engineering. His current research area is biosensor applications.

SIAO-JIE YAN was born in Hualien, Taiwan, in 1991. He received the bachelor's degree from the Department of Electro-Optical Engineering, National Formosa University, Yunlin, Taiwan, in 2014, and the master's degree from the Graduate School of Electronic Engineering, National Yunlin University of Science and Technology, Yunlin, Taiwan, in 2017. His research interest includes the biosensors included their applications and characterization.

CIAN-YI WU was born in Kaohsiung, Taiwan, in 1994. She received the B.S. degree in electro-optical engineering from the Southern Taiwan University of Science and Technology, Tainan, Taiwan, in 2016, and the M.S. degree in electronic engineering from the National Yunlin University of Science and Technology, Yunlin, in 2018. Her research interest includes the biosensors included their applications and characterization.